THE JOURNAL OF PHYSICAL CHEMISTRY C

Article

pubs.acs.org/JPCC

Mechanism of Photochemical Phase Transition of Single-Component Phototropic Liquid Crystals Studied by Means of Holographic Grating Recording

Anna Sobolewska,*[,†] Joanna Zawada,[†] Stanislaw Bartkiewicz,[†] and Zbigniew Galewski[‡]

[†]Institute of Physical and Theoretical Chemistry, Wroclaw University of Technology, Wybrzeze Wyspianskiego 27, 50-370 Wroclaw, Poland

[‡]Faculty of Chemistry, University of Wroclaw, Joliot-Curie 14, 50-383 Wroclaw, Poland

Supporting Information

ABSTRACT: Phototropic liquid crystals (PtLC) are a new class of materials possessing number of potential applications in photonics devices. However, so far a significant majority of PtLC materials has been realized by the doping a classical liquid crystal with a photochromic dye. The photochemical phase transition in such systems was investigated mainly by the monitoring of the changes in the transmittance. In this study, the photochemical phase transition of single-component phototropic liquid crystals was investigated using a holographic grating recording in combination with a polarized optical microscope. The *cis*−*trans* photoisomerization of compounds causes the isotropic-to-nematic (I−N) phase transition and so that the interference pattern can be mapped as a diffraction grating. The process of the grating build up was monitored by the first-order light diffraction, and simultaneously the area of the material exposed to the light was observed directly under a polarized microscope. The combination of the holographic technique with polarized optical microscopy has allowed to propose the mechanism of the I−N phase transition of LC compounds. It assumes three processes responsible for the grating formation. The results have a crucial importance in understanding the mechanism of photochemical phase transition of PtLCs, and thus they can be useful in construction of new optical devices.

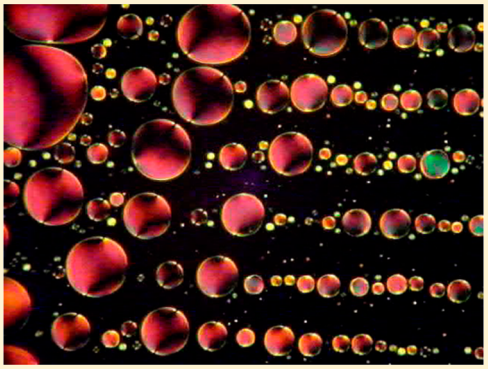

1. INTRODUCTION

Liquid crystals (LC) are widely used materials in daily life due to their unique properties. Traditional LCs are classified as thermotropic (TLC), which means that the temperature generates the mesophase, or lyotropic (LLC), in which mainly the concentration affects the phase transition.[1] In the past few years research is being conducted on a new class of LCs in which the phase transition is induced by the light.[2−20] Such materials are called phototropic liquid crystals (PtLC), and they open a new way for applications of liquid-crystalline materials in the photonic devices fully controlled by the light.[4,7,21]

Most PtLCs have been realized by the doping a classical LC with a photochromic dye. The photochemical reaction of the photochromic molecule dispersed in a LC matrix induces changes in the alignment of the liquid-crystalline host which can lead to the phase transition, called a photochemical phase transition.[5,6,13] Among many different photochromic compounds, the azobenzene derivatives seem to be exploited the most.[2−4,6,12,13,16,20] The photoisomerization process of the azobenzene is accompanied by a significant change in the molecular shape from an elongated rod-like *trans*-form into a bent banana-like *cis*-form which has been used to control the ordering of the LC molecules. The *trans*-isomer, due to its elongated shape, stabilizes the LC phase whereas the bent *cis*-isomer destabilizes the LC phase.[7] Therefore, the phase transition from the nematic-to-isotropic (N−I) (*order-to-disorder*) or from the isotropic-to-nematic (I−N) (*disorder-to-order*) can be induced isothermally by the *trans*−*cis* or *cis*−*trans* photoisomerization of the azobenzene derivatives, respectively. Generally speaking, the phase transition of the LCs can be controlled by the light.

The photochemical phase behavior of azobenzene LCs was already studied in the transmission,[7,12,13,16,22−26] reflection,[27−29] and scattering mode.[30,31] Besides that, the formation of holographic gratings by means of the photochemical phase transition was also reported although only in the case of polymer LCs containing azobenzene moieties.[32−39] So far, it was determined that the grating formed in these materials is a phase type grating and results from large modulation of the refractive index in the material arising from the difference in the refractive index between the nematic phase and the isotropic one, which is the undisputed finding. The holographic grating recording is a technique which is a very sensitive to any changes in the material properties, in which diffraction of light provides

Received: March 30, 2013
Revised: April 15, 2013
Published: April 18, 2013

information about these changes;[40−42] therefore, it is an excellent tool to investigate in detail what kinds of processes are occurring during the phase transition. However, a full description of these processes cannot be done when using this technique alone.

In this article, we investigated the photochemical phase transition of single-component phototropic liquid crystals from the family of 4-heptyl-4′-alkoxyazobenzene by means of the holographic grating recording combined with the polarized optical microscope. As a result of the *cis*−*trans* photoisomerization, the I−N phase transition of the compound was finally induced in the system. The whole process from the beginning, i.e, when the laser irradiation was turned on, until the occurrence of the phase transition was monitored by the light diffraction, and simultaneously the area of the material exposed to light was observed directly under the polarized microscope. By applying the combination of the holographic technique with polarized optical microscopy, we were able to identify the processes occurring during the phase transition. On the basis of the diffraction efficiency dynamics curves and microscopic observations, we proposed the mechanism of the I−N phase transition of the LC compounds. It assumes three processes responsible for the grating formation. The times of the beginnings of these processes depended on the chemical structure of the liquid crystals, i.e., on the length of the alkoxy chain.

2. EXPERIMENTAL SECTION

2.1. Materials. Single-component phototropic liquid-crystalline compounds are based on derivative of azobenzene. The family of 4-heptyl-4′-alkoxyazobenzene (7-AB-O*n*) for the alkoxy chain (*n*) from methoxy to hexyloxy (*n* = 1−6) was synthesized as reported previously.[43] The general chemical formula of 7-AB-O*n* is shown in Figure 1.

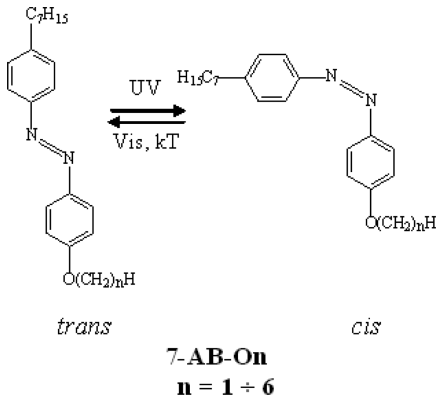

Figure 1. Chemical structure of the family of 4-heptyl-4′-alkoxyazobenzene liquid crystals (7-AB-O*n*, *n* = the number of carbon atoms of the alkoxy chain) and *trans*−*cis* isomerization of 7-AB-O*n*.

2.2. Characterization of the LCs. Liquid-crystalline behavior and phase transition behavior were examined on a polarized optical microscope (Olympus, BX600P) equipped with a hot stage (Linkam, l THMS 600) and a control unit (TMS 93). The thermotropic properties were determined using a differential scanning calorimeter (DSC, PerkinElmer DSC7) at a heating rate of 5 °C/min. The photoisomerization behavior of 7-AB-O3 was observed with a UV−vis absorption spectrometer (Cary 3, Varian Techtron).

2.3. Preparation of the LC Cells. The material (in the form of powder) was placed between two glass substrates (without any ordering layers) and heated above its isotropization temperature (T_i). The capillary forces caused the uniform distribution of the material within the cell. After the cooling the cell was closed. The spacers were not needed. The thickness of the cell was ca. 4 μm.

2.4. Photochemical Phase Transition Behavior. The holographic grating recording technique in combination with a polarized optical microscope was applied to examine the photochemical isotropic-to-nematic (I−N) phase transition in the family of 7-AB-O*n*. The experimental setup is shown in Figure 2.

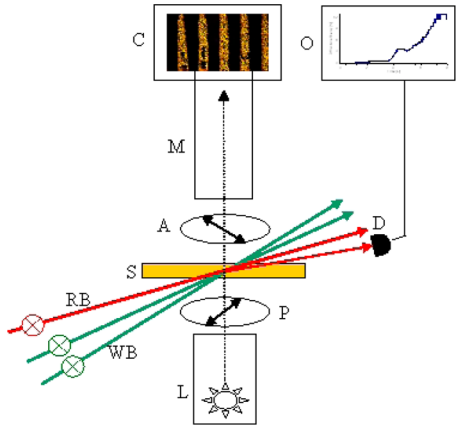

Figure 2. Schematic illustration of the experimental setup: L, white light source; S, sample; M, microscope; C, camera; D, detector; O, oscilloscope; WB, writing beams (marked the polarization state of the beams, s−s polarization configuration); RB, reading beam (s-polarized); P, polarizer; A, analyzer (arrows indicate the transmission axes of P and A).

The diffraction grating was written by two s-linearly polarized laser beams of the Nd:YAG laser (Coherent) operating at 532 nm (WB beams in Figure 2). The angle between the writing beams was fixed at ca. 0.5° resulting in a grating period of $\Lambda \cong 50$ μm. Intensities of the interfering beams were the same and equal to ca. 250 mW/cm^2. A linearly polarized He−Ne laser beam (633 nm, s-polarized) with low power was used as a reading beam at the angle of ca. 5° (RB beam in Figure 2). The polarized microscope equipped with a camera was placed right above the sample (M, C, and S, respectively, in Figure 2). The grating formation process was monitored by measuring the intensity of the first-order diffraction signal of the reading beam in a function of time. The multiple-order light diffraction was observed indicating the case of a Raman−Nath light scattering regime. The signal was measured with a photodiode (Thorlabs PDA 55) and registered by the oscilloscope (Tektronix TDS 2024B). The diffraction efficiency was determined by the ratio between the intensities of the first-order diffracted beam and the incident beam. Simultaneously, the grating recording process was directly observed under the polarized optical microscope and registered by the camera. The experiments were performed at room temperature.

3. RESULTS AND DISCUSSION

3.1. Characterization of the LCs. The phase transition temperatures of 7-AB-O*n* compounds are collected in Table 1. The strong even−odd effect of clearing temperatures was

dx.doi.org/10.1021/jp403159w | J. Phys. Chem. C 2013, 117, 10051−10058

Table 1. Thermotropic Properties of the Investigated Phototropic Liquid-Crystalline Compounds

compound	phase type and transition temp[a] (°C)
7-AB-O1	Cr 18.7 N 62.9 I
7-AB-O2	Cr 38.3 N 88.1 I
7-AB-O3	Cr 23.8 N 72.9 I
7-AB-O4	Cr 33.4 N 81.4 I
7-AB-O5	Cr 26.8 N 75.1 I
7-AB-O6	Cr 41.2 N 82.8 I

[a]Cr, crystal phase; N, nematic phase; I, isotropic phase.

detected. With increasing length of the alkoxy chain the isotropization temperature was found to increase in the case of the odd number of carbon atoms of the alkoxy chain, whereas for the even number it rather decreased.

The alkylalkoxyazobenzene liquid crystals present a reversible isomerization process between two isomers *trans* and *cis*. The *trans*-to-*cis* isomerization takes place by irradiation with UV light while the *cis*-form can be converted back to *trans* either by irradiation with the visible light or simply by the thermal relaxation (cf. Figure 1). The exemplary absorption spectrum of 7-AB-O3 in chloroform is shown in Figure 3.

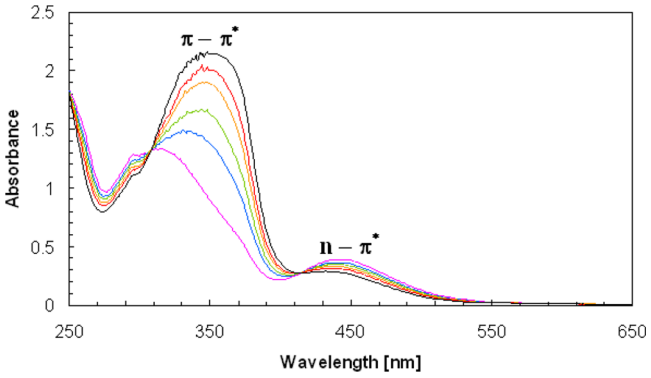

Figure 3. UV−vis absorption spectrum of 4-heptyl-4′-propoxyazobenzene (7-AB-O3) in chloroform ($C = 1.5 \times 10^{-4}$ mol dm^{-3}) before UV exposure (black line) and a change in the spectrum after UV irradiation at wavelength 365 nm (UV lamp, 100 W, 10 min, pink line). The other lines correspond to the thermal relaxation (from the pink line to black one). The recovery of the initial spectrum (black line) occurs after the time of 45 min.

Before UV light exposure, the spectrum is characterized by the absorption maxima at about 344 nm and at about 440 related to strong $\pi-\pi^*$ and weak n$-\pi^*$ transition bands of the *trans*-azobenzene mesogen, respectively. Irradiation by the light from a range of the $\pi-\pi^*$ transition band (365 nm in the current study) induces the *trans*−*cis* isomerization establishing a steady state between the thermodynamically stable *trans*-form of the azobenzene mesogen and its metastable *cis*-form. As a result, the intensity of the $\pi-\pi^*$ transition band at 344 nm gradually decreases, and simultaneously the intensity of the n$-\pi^*$ transition band at 440 nm, assigned to the *cis*-azobenene mesogen, gradually increases until the photostationary state is obtained (Figure 3). The system becomes rich in *cis*-isomers. Subsequent illumination by the light from a range of the n$-\pi^*$ transition band would induce the *cis*−*trans* isomerization and would lead to the establishment of a new steady state rich in *trans*-isomers.

3.2. Isothermal Phase Transition. After the preparation procedure, the LC cell contained the material in the crystal state comprised of the molecules in the *trans*-form. Since in the present work we investigate the photochemical isotropic-to-nematic (I−N) phase transition by means of the holographic grating recording, the cell had to be first brought into the isotropic phase. In order to do that, it was subjected to the irradiation by the light at the wavelength $\lambda = 365$ nm. Since the light was from the range of the $\pi-\pi^*$ transition band, the *trans*−*cis* isomerization was induced in the system, and thus the *cis*-form started to be generated. The appearing of the bent banana-like *cis*-form initiated the generation of the disorder in the system. The longer illumination, the higher population of the *cis*-isomer and thereby higher disorganization of the structured phase which in consequence led to the reduction of the Cr−N and N−I phase transitions temperatures and finally resulted in the isothermal phase transition (room temperature) from the crystal phase to the isotropic phase. The cell being in the isotropic phase (rich in the *cis*-form) was ready to use in the grating recording experiment.

3.3. Dynamics of the Grating Formation. Figure 4 shows the changes in the diffraction efficiency as a function of time during the exposure to the spatial light intensity modulation obtained for the family of 7-AB-O*n* at room temperature.

Three stages of the grating formation process can be distinguished on the basis of the behavior of the diffraction efficiency dynamics curves. The characteristic points on the time scale 0, t_a, t_b, t_c, and t_d, connected with the beginning of each stage, are indicated in Figure 5 in which the diffraction efficiency dynamics for 7-AB-O3 is depicted. t_a is the accommodation time, i.e., the time after which the light diffraction started to be observed, and t_d is the time after the diffraction efficiency reached the maximum. The times t_b and t_c were determined using a Raman−Nath light scattering regime by the applying the equation for the diffraction efficiency (η):

$$\eta_x = J_1^2(\phi_m(1 - e^{-k_x(t-t_x)})), \quad x = \text{b or c} \tag{1}$$

where J_1 is the first-order Bessel function, ϕ_m is the maximum amplitude of the process, k_x is the rate constant, and t_x is the time of the beginning of the process. These times for all compounds from the family are collected in Table 2.

In our experiment the grating formation process was not only monitored by measuring the light intensity of the diffraction signal, but it was simultaneously observed in real time under the polarized microscope and recorded by the camera. The observation of the material, which was exposed to light, under the polarized microscope provided the information about its LC structure phase in the specific time of the grating recording process. Both measurements of the diffraction efficiency dynamics and the recording of the movie about the phase occurring in the cell (see Supporting Information) started at the same time, that is, when the writing process was turned on.

Figure 6 presents the polarized optical micrographs of the LC cell during the process of the diffraction grating formation in 7-AB-O3. On the basis of the movie, we were able to determine the exact time (t_m) for which the first liquid-crystalline domains began to form, thereby when the I−N phase transition occurred. Such analysis was performed for all investigated liquid crystals, and the time t_m is collected together

dx.doi.org/10.1021/jp403159w | J. Phys. Chem. C 2013, 117, 10051−10058

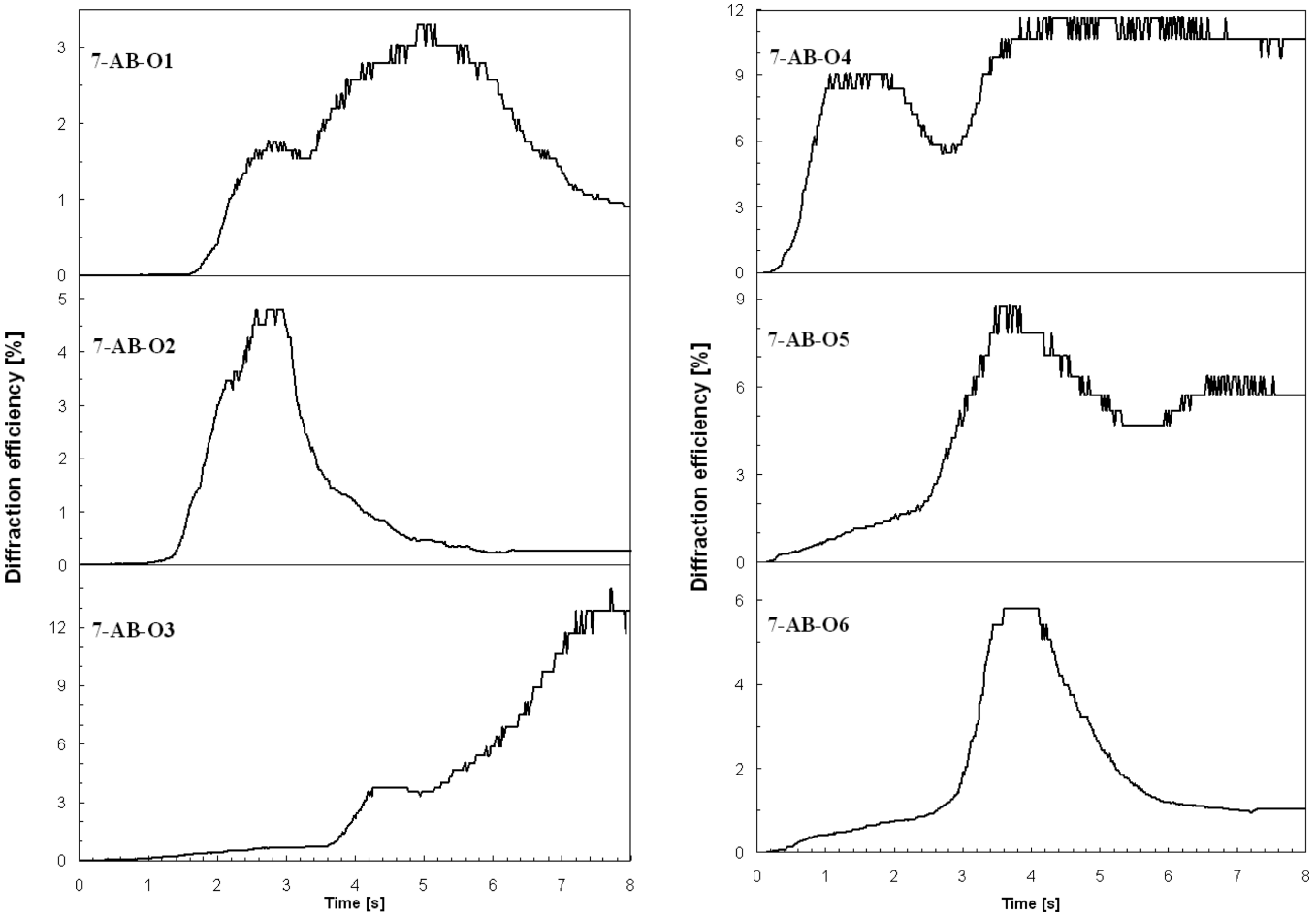

Figure 4. Diffraction efficiency as a function of time measured during the holographic grating recording process in the family of 7-AB-O*n* at room temperature.

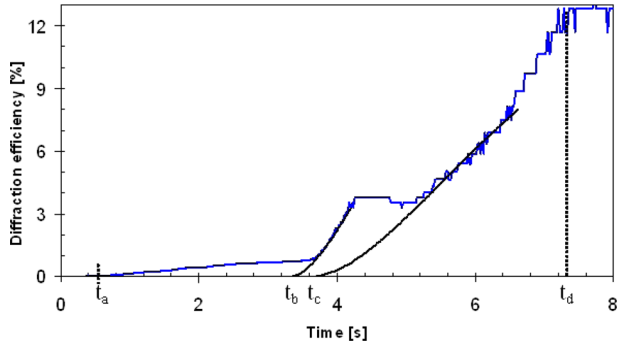

Figure 5. Diffraction efficiency in function of time measured during the holographic grating recording process in 7-AB-O3 for which the characteristic points (t_a, t_b, t_c, and t_d) were indicated (see text for details). The times t_b and t_c were determined based on eq 1.

Table 2. Times of the Beginnings of the Formation Process of the Respective Gratings

compound	alkoxy chain length	beginnings of the formation process of the gratings (s)				
	n	t_a	t_b	t_c	t_m	t_d
7-AB-O*n*	1	1.4	1.4	1.4	1.39	4.2
	2	1	1.2	1.3	1.25	2.6
	3	0.6	3.3	3.6	3.41	7.3
	4	0.2	0.4	2.6	2.47	4.3
	5	0.1	2.1	3.6	3.48	6.4
	6	0.1	0.6	2.6	2.53	4.0

with times obtained from the diffraction efficiency dynamics curves in Table 2.

Let us discuss in details what was happening during the grating formation process based on the results obtained for 7-AB-O3 and shown in Figures 5 and 6. When the process of the grating formation was started, the diffraction signal was close to zero until the time t_a. Next, the slow increase in the diffraction efficiency started at t_a which indicated that something enabling the weak diffraction of light was initiated in the cell. The slow increase was followed by the rapid increase in the diffraction efficiency began at t_b. This was caused by some other process and clearly pointed out the next stage of the grating formation process. However, this increase started to be erasure by the appearing of another process which started at t_c and was reflected in the significant increase in the diffraction efficiency. The system reached the maximum diffraction efficiency at t_d. On the basis of the microscopic observation, one can see that until the time t_m only the isotropic phase existed in the system (Figure 6A). The phase transition occurred at t_m (Figure 6B). It generated the formation of the phase diffraction grating which amplitude was increasing with the time until t_d (Figure 6C). Comparing the results obtained from the observation under the microscope with those from the diffraction efficiency dynamics, it turned out that t_m is equal to t_c (cf. Table 2). Keeping in mind

dx.doi.org/10.1021/jp403159w | J. Phys. Chem. C 2013, 117, 10051−10058

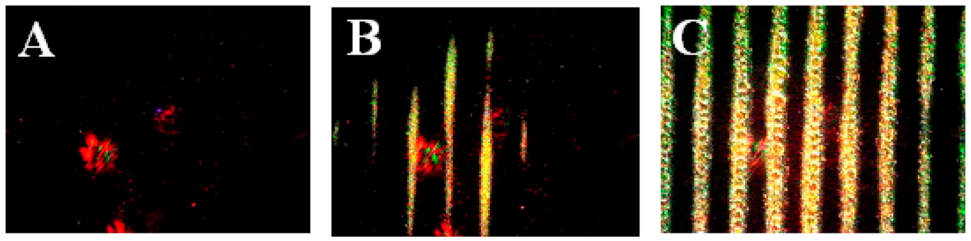

Figure 6. Polarized optical micrographs of the LC cell filled with the PtLC material during the process of the holographic grating formation for different time: (A) $0 \leq t < t_m$, (B) $t = t_m$, and (C) $t = t_d$ (see also Supporting Information).

that before the time t_c there were three other stages distinguished in the process of the grating formation clearly observed by the diffraction of light, there is no doubt that the behavior of the diffraction efficiency before t_c provides the essential information about what was happening before the I–N phase transition. Therefore, only the combination of the experiment of the diffraction grating recording with the direct observation of the grating formation process under the polarized microscope has brought to a new insight into the mechanism of the photochemical phase transition of the LC compounds.

3.4. Mechanism of the Grating Formation Based on the Photochemical Phase Transition of Phototropic Liquid Crystal. Three stages of the grating formation process in the family of 7-AB-O*n* were distinguished on the basis of the diffracted signal (cf. Figure 4 or 5) and described by the respective times (t_a, t_b, and t_c). Since the process of the grating formation was simultaneously observed under the polarized microscope, the exact time (t_m) when the first liquid-crystalline domains began to form (the beginning of the I–N phase transition) had been determined independently. The comparison of the results has brought to the conclusion that t_c is equal to t_m. All the times are collected in Table 2. Moreover, Figure 7A,B illustrates the behavior of the times in the function of the alkoxy chain length, whereas Figure 7C shows the dependence of the isotropization and crystallization temperatures (Table 1) also in the function of the alkoxy chain. The mechanism of the photochemical I–N phase transition of 7-AB-O*n* on the basis of the formation of the diffraction grating is schematically illustrated in Figure 8. Turning on the writing process (t = 0) initiated the *cis–trans* isomerization in the cell in the bright regions of the interference pattern (reminding, the wavelength of the writing beams was 532 nm which laid in the n–π^* transition band). The population of the *cis*-molecules was still large, which prevented the ordering of the *trans*-molecules (Figure 8A). Right after the accommodation time (t_a) a slow increase in the diffraction efficiency was observed (cf. Figure 5, the time range from t_a to t_b) which was connected with the formation of the absorption grating G_a. The G_a results from the changes in the orientation of the molecules in the isotropic phase due to the *cis–trans* isomerization (Figure 8B). After t_a the concentration of the molecules in the *trans*-form was big enough to cause the collective isomerization of the molecules, which led to the significant increase in the reaction rate observed as an absorption grating formation. One can see in Figure 7A that t_a was shorter for the longer alkoxy chains (it changed from 1.4 s for n = 1 to 0.1 s for n = 6); thereby the G_a formed faster in the case of 7-AB-O*n* with higher number of carbon atoms in the alkoxy chain (the longer molecule in the *trans*-form causes the higher ordering). The absorption grating can exceed the diffraction efficiency above 2% (Figure 4, 7-AB-O5). The continuous *cis–trans* isomerization led to increase in the *trans*-molecules population; as a result, the local areas with the same spatial arrangement of the *trans*-molecules (forced by their elongated shape) started to be formed in the system (Figure 8C). Thereby the refractive index of the system was locally changed, and the phase grating G_b started to be built up. Such ordered areas were getting larger, and after exceeding the critical point (the time t_c) they started to formed nematic domains (Figure 8D). The creation of LC domains was the origin of the grating G_c which in fact was formed on the basis of the direct neighborhood between the isotropic phase and the nematic phase. Thereby the significant increase in the diffraction efficiency was observed from the time t_c which resulted from the increasing difference in the refractive index between the isotropic and nematic phases (the difference is meaningful). The formed LC domains reflect the interference pattern. Since the growth of the domains starts in the areas with the highest light intensity and the transverse dimension of the forming diffraction grating grows up, an increase in the diffraction efficiency was observed. The maximum diffraction efficiency was observed for domains which size equals the half of the light intensity period (it corresponds to the time t_d, cf.

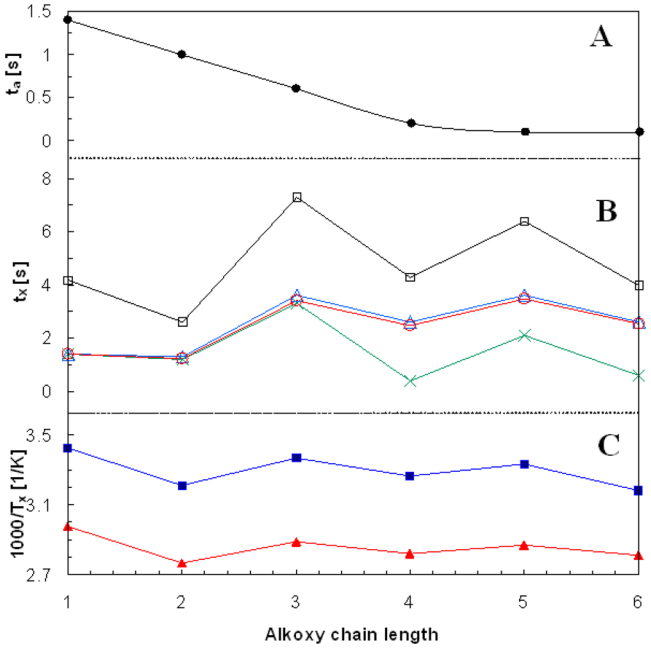

Figure 7. Dependences of the times of the beginnings of the formation process of the respective gratings (G_a, G_b, and G_c) and isotropization and crystallization temperatures (T_i and T_c) as a function of the alkoxy chain length: (A) t_a, (B) t_x, x = b (green cross symbol), c (blue triangle symbol), d (black square symbol), and m (red circle symbol); (C) T_x, x = i (red triangle symbol) and c (blue square symbol).

dx.doi.org/10.1021/jp403159w | J. Phys. Chem. C 2013, 117, 10051–10058

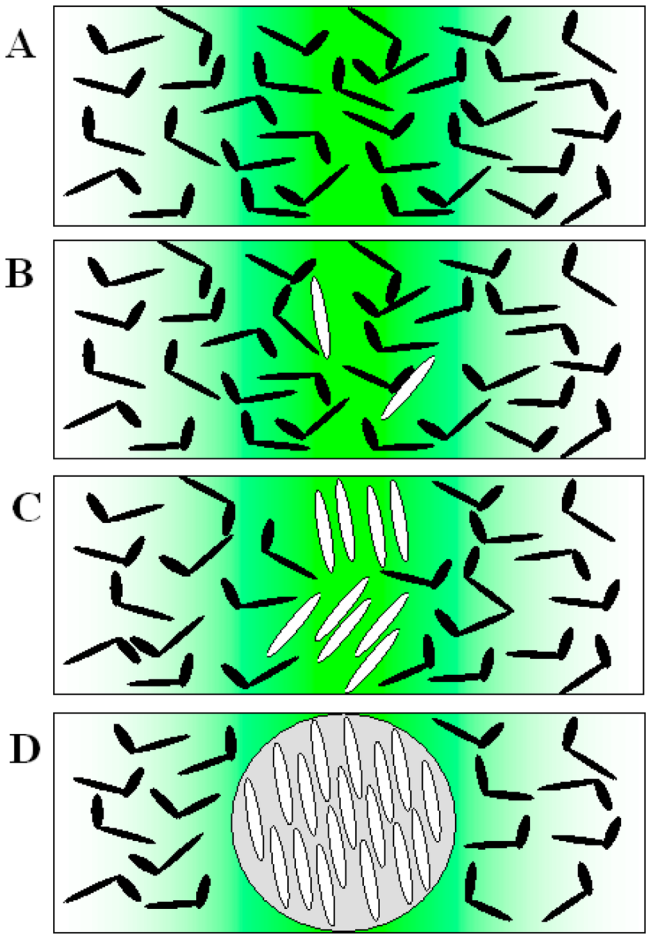

Figure 8. Schematic of the mechanism of the photochemical phase transition of 7-AB-O*n* and preceding processes it: (A) turning on the laser irradiation and initiation of the *cis*−*trans* isomerization in the bright regions of the interference pattern; (B) changes in the orientation of the molecules in the isotropic phase due to the *cis*−*trans* isomerization, G_a; (C) increased population of the molecules in the *trans*-form results in formation of the local areas with the same spatial arrangement of the trans-molecules, G_b; (D) these areas become bigger and when they exceed the critical point they started to form nematic domains, G_c.

Figure 5). If the recording process is not stopped at t_d, the further increase in the transverse domains size would be observed which in the critical case can lead to the complete disappearance of the diffraction efficiency; in other words, the size of domains would be equal to the period (Figure 4, 7-AB-O2).

Dynamics of each process depends strongly on the chemical structure of the 7-AB-O*n* as it can be seen in Figure 7. The time of the beginning of the G_a formation process was inversely proportional to the length of the alkoxy chain (cf. Figure 7A), whereas in the case of formation of G_b and G_c the times of the beginnings of these processes show the even−odd when the length of the alkoxy chain increases (Figure 7B). The even−odd effect correlates well with the even−odd effect observed for the isotropization (T_i) and crystallization (T_c) temperatures depicted in Figure 7C. One can see that for n = 1 the times of the beginnings of the formation of G_b and G_c where the same, but for the longer alkoxy chain these times started to be separated. Beside that it was noticed that the times were inversely proportional to the intensity of the writing beams, which will be the subject of the further studies. Moreover, the results show that in order to obtain the fastest recording of the phase type, the compounds with short alkoxy chain should be taken. In contrast, in order to get fast recording of the amplitude type (the lower diffraction efficiency), the compounds with longer alkoxy chain (n = 5, 6) should be considered.

Taking all into account, the investigation of the light-induced phase transition by means of holographic grating recording enabled to distinguish the processes occurring during the I−N phase transition. The initiated *cis*−*trans* isomerization resulted first, after the accommodation time, in the formation of absorption grating G_a, followed next by the formation of the phase grating G_b, based on the locally ordered *trans*-molecules, and finally led to the I−N phase transition and formation of the phase grating G_c, based on the neighborhood between the isotropic phase and the nematic phase.

It is worth mentioning that high diffraction efficiency (above 10%) was obtained for the investigated compounds at room temperature. The process was fully reversible (the subject of another paper). The diffraction grating can be completely erasure by applying the light at wavelength below 400 nm.

4. CONCLUSION

The photochemical phase transition of single-component PtLCs from the family of 4-heptyl-4′-alkoxyazobenzene by means of the holographic grating recording combined with the polarized optical microscope has been studied. By applying these techniques together, the processes occurring during the I−N phase transition were able to be identified. The mechanism of the phase transition of the LC compounds has been proposed which assumes three processes responsible for the grating formation. The formation of the phase grating, resulting from the difference in the refractive index between the nematic phase and the isotropic one, was preceded by the formation of the other phase grating, having a different origin than the previous one, and formation of the absorption grating. The times of the beginnings of the formation of the respective gratings depended on the length of the alkoxy chain.

It is worth to underline that phototropic LCs are characterized by the very fast response time, high efficiency, reversibility, and the full controlling by means of the light what makes them very competitive with the classical photorefractive LCs. Among the PtLCs the systems comprised a single-component PtLC have the unquestionable advantage over the doped ones since all the problems connected with the compatibility when mixing two different components (solubility, concentration) are ruled out. More importantly, PtLCs from the family of alkylalkoxyazobenzene can be easily chemically modified which makes possible to design materials with desired properties (polymorphism, phase transitions temperatures, optical density) on the molecular level. Taking all these into account, there is no doubt that the understanding the mechanism of the photochemical phase transition of the PtLC and all processes occurring during have a crucial importance both in developing new materials and in the construction of novel photonic devices based on single-component PtLC. These materials can find application in a wide class of photonic devices replacing materials used so far; i.e., photorefractive and photochromic polymers, liquid crystals, or nonlinear optical crystals especially can be applied as a permanent and dynamic optical memories.

dx.doi.org/10.1021/jp403159w | J. Phys. Chem. C 2013, 117, 10051−10058

■ ASSOCIATED CONTENT

Supporting Information

Movie of the LC cell filled with the PtLC material during the process of the holographic grating formation taken from the polarized optical microscope. This material is available free of charge via the Internet at http://pubs.acs.org.

■ AUTHOR INFORMATION

Corresponding Author

*Phone (048) 71 320 39 24; Fax (048) 71 320 33 64; e-mail anna.sobolewska@pwr.wroc.pl (A.S.).

Notes

The authors declare no competing financial interest.

■ ACKNOWLEDGMENTS

The work was performed under Grant 2011/01/B/ST8/03317 from the Polish National Science Centre.

■ REFERENCES

(1) Collings, P.; Hird, M. *An Introduction to Liquid Crystals: Chemistry and Physics*; Taylor and Francis: London, 1997.
(2) Sackmann, E. Photochemically Induced Reversible Color Changes in Cholesteric Liquid Crystals. *J. Am. Chem. Soc.* **1971**, *93*, 7088−7090.
(3) Pelzl, G. Conversion of a Nematic Phase into Isotropic Phase by Photochemical Isomerization. *Z. Chem.* **1977**, *17*, 294−295.
(4) Tazuke, S.; Kurihara, S.; Ikeda, T. Amplified Image Recording in Liquid Crystal Media by Means of Photochemically Triggered Phase Transition. *Chem. Lett.* **1987**, *16*, 911−914.
(5) Kurihara, S.; Ikeda, T.; Tazuke, S.; Seto, J. Isothermal Phase Transition of Liquid Crystals Induced by Photoisomerization of Doped Spiropyrans. *J. Chem. Soc., Faraday Trans.* **1991**, *87*, 3251−3254.
(6) Legge, C. H.; Mitchell, G. R. Photo-Induced Phase Transitions in Azobenzene-Doped Liquid Crystals. *J. Phys. D: Appl. Phys.* **1992**, *25*, 492−499.
(7) Ikeda, T.; Tsutsumi, O. Optical Switching and Image Storage by Means of Azobenzene Liquid-Crystal Films. *Science* **1995**, *268*, 1873−1875.
(8) Dinescu, L.; Lemieux, R. P. Modulating the Spontaneous Polarization of a Ferroelectric Liquid Crystal via the Photoisomerization of a Chiral Thioindigo Dopant: (*R*,*R*)-6,6′-bis(1-methylheptyloxy) Thioindigo. *Liq. Cryst.* **1996**, *20*, 741−749.
(9) Dinescu, L.; Lemieux, R. P. Photomodulation of the Spontaneous Polarization of a Ferroelectric Liquid Crystal: Harnessing the Transverse Dipole Modulation of a Chiral Thioindigo Dopant. *J. Am. Chem. Soc.* **1997**, *119*, 8111−8112.
(10) Yokoyama, Y.; Sagisaka, T. Reversible Control of Pitch of Induced Cholesteric Liquid Crystal by Optically Active Photochromic Fulgide Derivatives. *Chem. Lett.* **1997**, *26*, 687−688.
(11) Denekamp, Ch.; Feringa, B. L. Optically Active Diarylethenes for Multimode Photoswitching Between Liquid-Crystalline Phases. *Adv. Mater.* **1998**, *10*, 1080−1082.
(12) Kurihara, S.; Yoneyama, D.; Nonaka, T. Photochemical Switching Behavior of Liquid-Crystalline Networks: Effect of Molecular Structure of Azobenzene Molecules. *Chem. Mater.* **2001**, *13*, 2807−2812.
(13) Sung, J. H.; Hirano, S.; Tsutsumi, O.; Kanazawa, A.; Shiono, T.; Ikeda, T. Dynamics of Photochemical Phase Transition of Guest/Host Liquid Crystals with an Azobenzene Derivative as a Photoresponsive Chromophore. *Chem. Mater.* **2002**, *14*, 385−391.
(14) Tamaoki, N.; Aoki, Y.; Moriyama, M.; Kidowaki, M. Photochemical Phase Transition and Molecular Realignment of Glass-Forming Liquid Crystals Containing Cholesterol/Azobenzene Dimesogenic Compounds. *Chem. Mater.* **2003**, *15*, 719−726.
(15) Davis, R.; Mallia, V. A.; Das, S. Reversible Photochemical Phase Transition Behavior of Alkoxy-Cyano-Substituted Diphenylbutadiene Liquid Crystals. *Chem. Mater.* **2003**, *15*, 1057−1063.
(16) Yu, Y.; Nakano, M.; Shishido, A.; Shiono, T.; Ikeda, T. Effect of Cross-Linking Density on Photoinduced Bending Behavior of Oriented Liquid-Crystalline Network Films Containing Azobenzene. *Chem. Mater.* **2004**, *16*, 1637−1643.
(17) Bobrovsky, A.; Shibaev, V.; Hamplova, V.; Kaspar, M.; Novotna, V.; Glogarova, M.; Pozhidaev, E. Photoinduced Phase Transitions and Helix Untwisting in the SmC* Phase of a Novel Cinnamoyl-Based Liquid Crystal. *Liq. Cryst.* **2009**, *36*, 989−997.
(18) Tamaoki, N.; Kamei, T. Reversible Photo-Regulation of the Properties of Liquid Crystals Doped with Photochromic Compounds. *J. Photochem. Photobiol. C: Photochem. Rev.* **2010**, *11*, 47−61.
(19) Kosa, T.; Sukhomlinova, L.; Su, L.; Bahman, T.; White, T. J.; Bunning, T. J. Light-Induced Liquid Crystallinity. *Nature* **2012**, *485*, 347−349.
(20) Wang, G.; Zhang, M.; Zhang, T.; Guan, J.; Yang, H. Photoresponsive Behaviors of Smectic Liquid Crystals Tuned by an Azobenzene Chromophore. *RSC Adv.* **2012**, *2*, 487−493.
(21) Ikeda, T. Photomodulation of Liquid Crystal Orientations for Photonic Applications. *J. Mater. Chem.* **2003**, *13*, 2037−2057.
(22) Tsutsumi, O.; Shiono, T.; Ikeda, T.; Galli, G. Photochemical Phase Transition Behavior of Nematic Liquid Crystals with Azobenzene Moieties as Both Mesogens and Photosensitive Chromophores. *J. Phys. Chem. B* **1997**, *101*, 1332−1337.
(23) Tsutsumi, O.; Kitsunai, T.; Kanazawa, A.; Shiono, T.; Ikeda, T. Photochemical Phase Transition Behavior of Polymer Azobenzene Liquid Crystals with Electron-Donating and -Accepting Substituents at the 4,4′-Positions. *Macromolecules* **1998**, *31*, 355−359.
(24) Tsutsumi, O.; Demachi, Y.; Kanazawa, A.; Shiono, T.; Ikeda, T.; Nagase, Y. Photochemical Phase-Transition Behavior of Polymer Liquid Crystals Induced by Photochemical Reaction of Azobenzenes with Strong Donor-Acceptor Pairs. *J. Phys. Chem. B* **1998**, *102*, 2869−2874.
(25) Kurihara, S.; Nomiyama, S.; Nonaka, T. Photochemical Switching Between a Compensated Nematic Phase and a Twisted Nematic Phase by Photoisomerization of Chiral Azobenzene Molecules. *Chem. Mater.* **2000**, *12*, 9−12.
(26) Kurihara, S.; Nomiyama, S.; Nonaka, T. Photochemical Control of the Macrostructure of Cholesteric Liquid Crystals by Means of Photoisomerization of Chiral Azobenzene Molecules. *Chem. Mater.* **2001**, *13*, 1992−1997.
(27) Shishido, A.; Tsutsumi, O.; Kanazawa, A.; Shiono, T.; Ikeda, T.; Tamai, N. Rapid Optical Switching by Means of Photoinduced Change in Refractive Index of Azobenzene Liquid Crystals Detected by Reflection-Mode Analysis. *J. Am. Chem. Soc.* **1997**, *119*, 7791−7796.
(28) Shishido, A.; Tsutsumi, O.; Kanazawa, A.; Shiono, T.; Ikeda, T.; Tamai, N. Distinct Photochemical Phase Transition Behavior of Azobenzene Liquid Crystals Evaluated by Reflection-Mode Analysis. *J. Phys. Chem. B* **1997**, *101*, 2806−2810.
(29) Shishido, A.; Kanazawa, A.; Shiono, T.; Ikeda, T.; Tamai, N. Enhancement of Stability in Optical Switching of Photosensitive Liquid Crystal by Means of Reflection Mode Analysis. *J. Mater. Chem.* **1999**, *9*, 2211−2213.
(30) Lee, H.-K.; Kanazawa, A.; Shiono, T.; Ikeda, T.; Fujisawa, T.; Aizawa, M.; Lee, B. All-Optically Controllable Polymer Liquid Crystal Composite Films Containing the Azobenzene Liquid Crystal. *Chem. Mater.* **1998**, *10*, 1402−1407.
(31) Lee, H.-K.; Kanazawa, A.; Shiono, T.; Ikeda, T.; Fujisawa, T.; Aizawa, M.; Lee, B. Reversible Optical Control of Transmittance in Polymer/Liquid Crystal Composite Films by Photoinduced Phase Transition. *J. Appl. Phys.* **1999**, *86*, 5927−5934.
(32) Hasegawa, M.; Yamamoto, T.; Kanazawa, A.; Shiono, T.; Ikeda, T. A Dynamic Grating Using a Photochemical Phase Transition of Polymer Liquid Crystals Containing Azobenzene Derivatives. *Adv. Mater.* **1999**, *11*, 675−677.
(33) Hasegawa, M.; Yamamoto, T.; Kanazawa, A.; Shiono, T.; Ikeda, T.; Nagase, Y.; Akiyama, E.; Takamura, Y. Real-Time Holographic

Grating by Means of Photoresponsive Polymer Liquid Crystals with a Flexible Siloxane Spacer in the Side Chain. *J. Mater. Chem.* **1999**, *9*, 2765−2769.
(34) Hasegawa, M.; Yamamoto, T.; Kanazawa, A.; Shiono, T.; Ikeda, T. Photochemically Induced Dynamic Grating by Means of Side Chain Polymer Liquid Crystals. *Chem. Mater.* **1999**, *11*, 2764−2769.
(35) Yamamoto, T.; Hasegawa, M.; Kanazawa, A.; Shiono, T.; Ikeda, T. Phase-Type Gratings Formed by Photochemical Phase Transition of Polymer Azobenzene Liquid Crystals: Enhancement of Diffraction Efficiency by Spatial Modulation of Molecular Alignment. *J. Phys. Chem. B* **1999**, *103*, 9873−9878.
(36) Yamamoto, T.; Yoneyama, S.; Tsutsumi, O.; Kanazawa, A.; Shiono, T.; Ikeda, T. Holographic Gratings in the Optically Isotropic State of Polymer Azobenzene Liquid-Crystal Films. *J. Appl. Phys.* **2000**, *88*, 2215−2220.
(37) Yamamoto, T.; Hasegawa, M.; Kanazawa, A.; Shiono, T.; Ikeda, T. Holographic Gratings and Holographic Image Storage via Photochemical Phase Transitions of Polymer Azobenzene Liquid-Crystal Films. *J. Mater. Chem.* **2000**, *10*, 337−342.
(38) Yoneyama, S.; Yamamoto, T.; Hasegawa, M.; Tsutsumi, O.; Kanazawa, A.; Shiono, T.; Ikeda, T. Formation of Intensity Grating in a Polymer Liquid Crystal with a Side-Chain Azobenzene Moiety by Photoinduced Alignment Change of Mesogens. *J. Mater. Chem.* **2001**, *11*, 3008−3013.
(39) Yamamoto, T.; Ohashi, A.; Yoneyama, S.; Hasegawa, M.; Tsutsumi, O.; Kanazawa, A.; Shiono, T.; Ikeda, T. Phase-Type Gratings Formed by Photochemical Phase Transition of Polymer Azobenzene Liquid Crystal. 2. Rapid Switching of Diffraction Beams in Thin Films. *J. Phys. Chem. B* **2001**, *105*, 2308−2313.
(40) Sobolewska, A.; Miniewicz, A. Analysis of the Kinetics of Diffraction Efficiency during the Holographic Grating Recording in Azobenzene Functionalized Polymers. *J. Phys. Chem. B* **2007**, *111*, 1536−1544.
(41) Sobolewska, A.; Bartkiewicz, S.; Miniewicz, A.; Schab-Balcerzak, E. Polarization Dependence of Holographic Grating Recording in Azobenzene-Functionalized Polymers Monitored by Visible and Infrared Light. *J. Phys. Chem. B* **2010**, *114*, 9751−9760.
(42) Czajkowski, M.; Bartkiewicz, S.; Mysliwiec, J. Growth of Isotropic Domains as a Mechanism of Dynamic Diffraction Grating Recording in Low Molecular Liquid-Crystalline Derivatives of Azobenzene. *J. Phys. Chem. B* **2012**, *116*, 3264−3269.
(43) Zienkiewicz, J.; Galewski, Z. Liquid Crystalline Properties of 4-Hexyl-4′-alkoxyazobenzenes and 4-Heptyl-4′-alkoxyazobenzenes. *Proc. SPIE* **1998**, *3319*, 45−54.